0026-895X/04/6602-209–219$20.00
MOLECULAR PHARMACOLOGY
Copyright © 2004 The American Society for Pharmacology and Experimental Therapeutics
Mol Pharmacol 66:209–219, 2004

Vol. 66, No. 2
3041/1163135
Printed in U.S.A.

Ligand-Binding Residues Integrate Affinity and Efficacy in the NMDA Receptor

Trisha L. Kalbaugh, Hendrika M. A. VanDongen, Antonius M. J. VanDongen

Department of Pharmacology and Cancer Biology, Duke University Medical Center, Durham, North Carolina

Received October 17, 2003; accepted April 26, 2004

This article is available online at http://molpharm.aspetjournals.org

ABSTRACT

The interaction of an agonist with its receptor can be characterized by two fundamental properties, affinity and efficacy. Affinity defines how tightly the agonist associates with its receptor, and efficacy measures the ability of the bound ligand to activate the receptor. Although affinity and efficacy are independent properties, the binding and activation processes that they describe are tightly coupled. This strong coupling has complicated the interpretation of concentration-response phenotypes caused by receptor mutations. We present an approach that quantifies the role of individual amino acids in defining affinity and efficacy. This method, which employs partial agonists and covalent modification of introduced cysteines, was applied to the ligand-binding sites of the NMDA receptor. Recent crystallographic structures for glutamate receptor ligand-binding cores allowed identification of residues that are either known or are predicted to be critical for ligand binding in the NR1 and NR2A subunit, respectively. Mutation of amino acids whose sidechains would directly coordinate bound ligands affected both agonist affinity and efficacy. In contrast, positions predicted to stabilize the closed-cleft conformation contributed only to agonist efficacy. The results provide a molecular basis for the tight coupling of agonist binding and receptor activation.

Agonists activate receptors in a multistep process that is initiated by a ligand binding reaction and culminates in conversion of the receptor to the active conformation. The molecular mechanisms underlying these events can be most rigorously studied in ligand-gated ion channels; activation of these receptors results in opening of the associated channel, which can be directly measured as an ionic current. In 1957, del Castillo and Katz proposed a minimal model describing agonist-dependent activation of ligand-gated ion channels. Their model consisted of two coupled equilibria that reflect binding and transduction (Fig. 1a). Agonist affinity is determined by the initial binding reaction, whereas the subsequent activation process sets agonist efficacy. Agonist-receptor interactions can be experimentally characterized by concentration-response curves. The midpoint of these curves (EC_{50}) is determined by both affinity and efficacy, because of the coupling of the binding and activation reactions (Fig. 1, a and b).

Site-directed mutagenesis of receptors is an important tool for identifying domains involved in ligand binding and for assigning specific functional roles to individual residues. Point mutations in a receptor's ligand binding domain may alter agonist affinity, efficacy, or both. Until now, however, it has not been possible to unambiguously interpret changes in concentration-response relationships caused by receptor mutations. The first problem, illustrated in Fig. 1c, is that a change in the EC_{50} caused by a mutation could result from an effect on agonist binding (affinity) or transduction (efficacy). The second complication is that an observed change in maximal response does not assure an effect on efficacy, because the mutation may have affected the expression level of the receptor by changing protein folding efficiency or stability. We have developed an approach that addresses both these problems and applied it to investigate affinity and efficacy contributions of residues in the glutamate and glycine binding sites of the NMDAR, a member of the ionotropic glutamate receptor family (Dingledine et al., 1999).

The crystallization of the ligand-binding domain (LBD) of NR1 and GluR2 in the absence and presence of ligands has provided significant insights into the molecular mechanism of agonist binding and receptor activation (Armstrong et al., 1998; Armstrong and Gouaux, 2000; Furukawa and Gouaux, 2003). The crystallized LBD consists of the S1 and S2 extracellular domains (Stern-Bach et al., 1994), which form two globular lobes connected by an interlobe hinge. Ligands bind to amino acids in the interlobe cleft and induce domain closure. This initial conformational change has been proposed to

This work was supported by National Institutes of Health grants NS31557 and MH61506 (to A.M.J.V.D.) and MH64282 (to T.L.K.).

ABBREVIATIONS: NMDAR, *N*-methyl-D-aspartate receptor; LBD, ligand binding domain; NMDA, *N*-methyl-D-aspartate; MTSEA, (2-aminoethyl-)methanethiosulfonate; GluR, glutamate receptor; DCS, D-cycloserine.

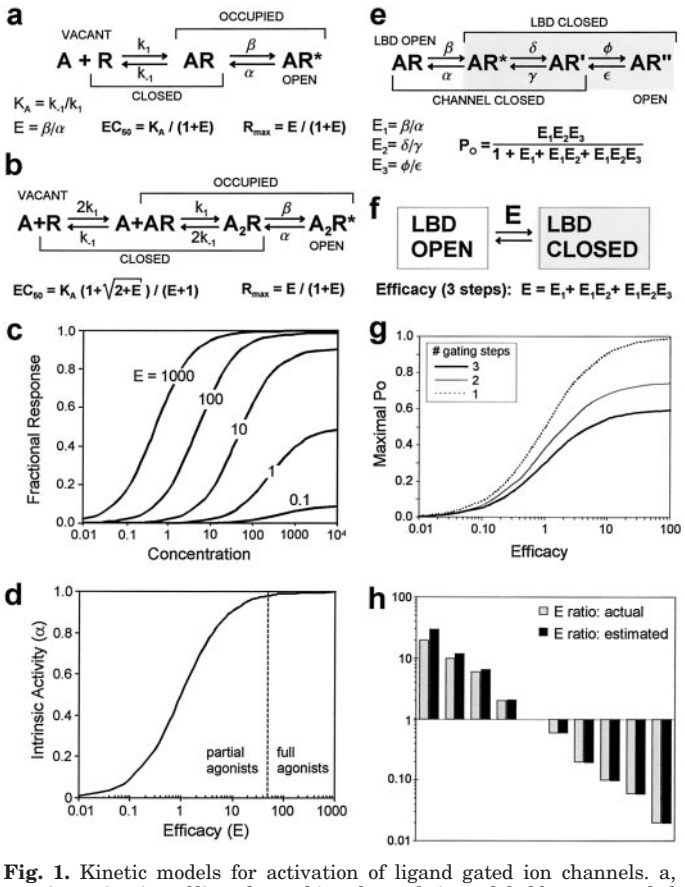

Fig. 1. Kinetic models for activation of ligand gated ion channels. a, agonist activation of ligand-gated ion channels is modeled by two coupled equilibria, according to del Castillo and Katz (1957). The first equilibrium describes the reversible binding reaction, in which the agonist associates with and dissociates from the ligand-binding site. The equilibrium constant associated with this reaction (K_A) measures agonist affinity. The second equilibrium describes the gating reaction in which the receptor moves between the resting (closed) and active (open) conformation. The equilibrium constant associated with this reaction (E) measures agonist efficacy. The equilibria are coupled by assuming that only occupied receptors are able to activate, thereby generating a linear, three-state model. [A] and [R] denote concentrations of ligand and free receptor, respectively; [AR] represents the concentration of ligand-bound, inactive receptor, and [AR*] is concentration of ligand-bound, active receptor. The equilibrium dissociation constant (K_A) is the ratio of the dissociation (k_{-1}) and association (k_{+1}) rate constants for ligand binding to the receptor. Following the convention of del Castillo and Katz (1957), K_A is referred to in this paper as the 'affinity constant', although it should be kept in mind that K_A is *inversely* proportional to the affinity. The efficacy constant (E) is the ratio of the forward (β) and reverse (α) rate constants for the conformational change induced by ligand binding. In this model, the maximum open probability (P_o) depends strictly on the value of E, but the EC_{50} is a function of both E and K_A. b, NMDA receptors are tetrameric assemblies of two NR1 and two NR2A subunits (Schorge and Colquhoun, 2003). As a result, there are probably two equivalent binding sites for each of the two coagonists, glycine and L-glutamate. To evaluate how the underlying kinetic model affects the calculated changes in affinity and efficacy constants, the model shown in a was expanded to include two binding-sites. The equations illustrate how the EC_{50} and maximum response (P_o) depend on the affinity and efficacy constants for this model. c, EC_{50} shifts for full agonists that are induced solely by changes in efficacy are not distinguishable from those induced by changes in affinity. Concentration-response relationships were generated using the 3-state model shown in a. The equilibrium dissociation constant K_A was maintained at a fixed value of 500, whereas the efficacy constant E was varied to values shown on the curves. Note that changes in maximal response are observable only for partial agonists (E values of approximately 50 and below), whereas for full agonists ($E > 50$), changing E results in a pure shift of the concentration response curve. d, the intrinsic activity as a function of the efficacy constant E is shown as a semi-log graph for the models shown in a and b. This relationship was used to estimate the E-value of a partial agonist from the experimentally determined intrinsic activity. e, this three-step gating model is an extension of the simple model shown in a. It describes a receptor in which three conformational changes are required to open the channel after agonist binding. Because the model is used here to calculate maximum open probability, supramaximal agonist concentration is assumed and there are therefore no unoccupied receptors ([R] = 0). The first equilibrium (E_1) describes events at the ligand binding domain (binding cleft closure), the second equilibrium (E_2) describes a putative intermediate transduction step coupling ligand binding to channel opening (Jones et al., 2002), the third equilibrium (E_3) describes events at the gate (channel opening). Maximum open probability (P_o) depends on E_1, E_2, and E_3, as shown. The equation can be generalized for n gating steps. Note that the LBD remains closed as the receptor moves between the states AR*, AR′, and AR″ indicated by a gray box. f, efficacy reflects the ability of the bound ligand to activate its receptor. Receptor activation involves conformational changes in the LBD, the transmembrane segments and the gate, resulting in a multistep activation cascade, as illustrated in e. However, agonists only interact with the LBD and consequently they are 'unaware' of any downstream conformational changes. Efficacy (E) is therefore determined by the equilibrium between two sets of conformations, for which the LBD is either open or closed. For the model in e with three activation steps, the efficacy constant is given by $E = E_1 + E_1E_2 + E_1E_2E_3$. g, to illustrate the relationship between open probability and efficacy, the maximum open probability is plotted as a function of E (see f), the efficacy equilibrium constant. In this example, efficacy was varied over four orders of magnitude by changing the value of the rate constant α while keeping the other microscopic rates constant: $\beta = 10$, $\gamma = 1$, $\delta = 3$, $\epsilon = 1$, and $\varphi = 2$. The values of the rate constants were chosen arbitrarily. However, the results are identical for any other choice of values. As can be seen from the graph, the maximum P_o for a full agonist ($E = 100$) decreases with increasing number of gating steps. Normalization for this value results in overlapping curves. The midpoint of the curves is always at $E = 1$, independent of the number of gating steps or the choice of rate constant values. This implies that the relationship between intrinsic activity (α) and efficacy (E), as shown in d, which we use to estimate E, is also independent of the number of gating steps. h, in the method developed here, the change in efficacy of a partial agonist induced by MTSEA modification is estimated. The model in a is used to convert intrinsic activity to an efficacy constant E. To evaluate the error introduced by this in our method, estimated and actual E-values after MTSEA were compared for the three-step gating model shown in e. Rate constants were set at the values given in g. It was assumed that the efficacy constant of the full agonist is 100 and that of the partial agonist is 1. Maximum open probabilities for the full and partial agonist were 0.583 and 0.300, respectively. The effect of MTSEA treatment was modeled by altering the rate constant α from an initial value of 60 to each of the following values: 3, 6, 10, 30, 100, 300, 600, 1000, and 3000. New E-values were calculated (f) and estimated from the intrinsic activity as described under *Materials and Methods*. As can be seen from the histogram, estimated E-values are very close to the actual values.

induce a subsequent movement of the transmembrane helices resulting in receptor activation (Armstrong and Gouaux, 2000; Jin et al., 2002; Sun et al., 2002). The closed cleft conformation of the LBD is stabilized by a group of six amino acids that form a nearly identical network of hydrogen bonds with all cocrystallized ligands (Armstrong and Gouaux, 2000; Mayer et al., 2001; Arinaminpathy et al., 2002; Furukawa and Gouaux, 2003). These amino acid residues were targeted in the NMDA receptor NR1 and NR2A subunits by a mutagenesis approach that allows the assessment of affinity and efficacy roles for each residue.

Materials and Methods

Mutations were generated using the megaprimer polymerase chain reaction method, as described previously (Wood et al., 1995), and were confirmed by DNA sequencing. cRNA for wild-type and mutant NMDAR subunits were prepared by in vitro transcription. Oocytes from adult female *Xenopus laevis* were prepared as described previously (VanDongen et al., 1990; Jones et al., 2002). Functional expression was assessed 2 to 5 days after injection using a two-electrode voltage clamp amplifier (OC-725; Warner Instruments, Hamden, CT) by application of agonists during continuous

perfusion of a buffer solution containing 100 mM NaCl, 5 mM KCl, 0.5 mM $BaCl_2$, 10 mM HEPES, and 10 μM EDTA, pH 7.3. Barium was substituted for calcium to minimize secondary activation of calcium-activated Cl^- currents (Leonard and Kelso, 1990). EDTA was used to chelate trace amounts of the divalent cations Cd^{2+} and Zn^{2+}, which have been reported to contaminate buffer solutions (Paoletti et al., 1995) and inhibit the NMDAR by binding to a high-affinity site (Paoletti et al., 1995). EDTA also removes a zinc-dependent component of desensitization (Zheng et al., 2001). Oocytes were placed in a perfusion chamber (Warner Instrument Corp., Hamden, CT) optimized for laminar flow. Solution changes were accomplished using a gravity-fed, computer-controlled perfusion system. Low-resistance glass microelectrodes (0.5–2.0 MΩ) were filled with 3 M KCl and 10 mM HEPES, pH 7.2, and used to impale the oocytes. Current traces were recorded from a holding potential of -60 mV. Data acquisition and voltage control was accomplished with pClamp hardware and software (Axon Instruments, Union City, CA). Oocytes expressing NMDA receptors were perfused with MTSEA HBr (0.5 mM, 60 s; Toronto Research Chemicals, North York, ON, Canada) to modify exposed thiol sidechains. After MTSEA treatment, oocytes were washed for 15 s with buffer before the next challenge with agonists. Concentration-response data were normalized to the maximum response elicited at saturating concentration of agonists. The maximum response depends on the number of functional NMDA receptors, the maximum open probability, the single channel conductance and the electrochemical driving force. MTSEA treatment is expected to only affect the open probability.

Curve Fitting. Data were fitted with the Hill equation: $R/R_{max} = 1/[1 + (EC_{50}/A)^{n_H}]$, where R is the response (NMDA current) for the given agonist concentration (A), R_{max} is the maximal response, n_H is the Hill coefficient, and EC_{50} is the concentration midpoint. The fit was generated by minimizing the residual sum of squares, using the Solver function in Microsoft Excel (Microsoft, Redmond, WA). Data from each oocyte were fit individually, and given EC_{50} values represent the mean ± S.E.M.

Calculation of Changes in K_A and E. Intrinsic activity (α) of a partial agonist was measured as the ratio of the maximal response elicited by the partial agonist to the maximal response elicited by the most efficacious agonist at the binding site (denoted as the full agonist). The efficacy of the partial agonist before MTSEA treatment (E_{before}) was estimated from the intrinsic activity as follows: $E_{before} = \alpha/(1 - \alpha)$. This calculation assumes that efficacy of the full agonist is large ($E > 50$), so that its intrinsic activity is near unity (Fig. 1d). The partial agonist maximal response after treatment (R_{after}) was defined as the ratio of the partial agonist response after MTSEA treatment to the full agonist response before treatment. This value was used to calculate the efficacy of the partial agonist after MTSEA treatment: $E_{after} = R_{after} / (1 - R_{after})$. The modification-induced change in E for a partial agonist was expressed as a ratio E_{after}/E_{before}. Affinity of partial agonists is determined by the equilibrium dissociation constant K_A, which was calculated before and after modification as $K_A = EC_{50} \times (1 + E)$. Because K_A is calculated from E, its accuracy is determined by that of E. The change in affinity is calculated as the ratio of the K_A values before and after modification.

An alternative two-site model containing two equivalent binding sites for the same agonist was used to investigate how sensitive the approach is to changes in the underlying kinetic scheme. The fold change in the efficacy constant for the 2-site model is the same as described above. The K_A for the 2-site model is: $K_A = \{EC_{50} \times [(1 + E)/(1 + \sqrt{(2 + E)})]\}$. Statistical significance ($P < 0.05$) of changes in K_A and E were determined using the Student's t test (Microsoft Excel).

Results

An approach was developed to allow evaluation of affinity and efficacy roles for individual amino acid positions in a receptor LBD. Because agonist efficacy determines degree of receptor activation, a change in maximal response can reveal an efficacy phenotype for a mutation. However, variation in receptor expression levels between individual cells makes it difficult to reliably measure small differences in maximum response. Even if a mutation causes a statistically significant difference in maximal agonist response, one cannot draw a firm conclusion regarding a change in efficacy, because protein folding or stability may have been compromised. One possible solution would be to record single channel behavior and compare maximum open probabilities for wild-type and mutant receptors. Here, we have used an alternative solution that is compatible with macroscopic current measurements. The method uses an in situ mutagenesis approach, which employs covalent modification of substituted cysteines (Akabas et al., 1992). By covalently conjugating a bulky moiety to the introduced cysteine, reagents such as MTSEA can further affect the function of the mutated position without inducing misfolding or changing the receptor number. This approach allows the same receptor population to be studied before and after modification of the targeted amino acid. Concentration-response curves generated before and after MTSEA treatment can be compared to reliably assess the effects of modification on EC_{50} and maximal response. Even small changes in maximal response can then be unambiguously interpreted as effects on agonist efficacy.

However, mutation-induced changes in efficacy do not always alter the maximum response. This complication results from the fact that the maximum response is a hyperbolic function of efficacy (Fig. 1d). When the initial efficacy is very high, even a substantial decrease caused by a receptor mutation may not produce a measurable reduction in the maximum response. Instead, such a mutation will cause only a shift of the concentration response curve and concomitant increase in the EC_{50} (Fig. 1c). Because the efficacy of a full agonist cannot be empirically determined, it is not possible to evaluate the magnitude of this complication for any given agonist-receptor combination. This second problem was addressed by employing partial agonists, for which the relative efficacy can be estimated from their intrinsic activity (Ariens, 1954), which can be experimentally determined. For a partial agonist, any change in efficacy induced by a mutation should alter the maximum response.

The two complications described above were circumvented by a combination of in situ mutagenesis and the use of partial agonists. Full and partial agonist concentration-response relationships are generated for cysteine-substituted receptor mutations before and after treatment with MTSEA. The intrinsic activity of the partial agonist, together with the modification-induced changes in maximal response and EC_{50} are then used to calculate changes in the efficacy and affinity constants (see *Materials and Methods* and Fig. 1). The changes in affinity and efficacy are expressed as ratios (after/before MTSEA) of the corresponding constants, K_A and E. The E-ratio is relatively insensitive to the underlying gating model (Fig. 1, e-h). The robustness of the affinity ratio is discussed below.

Selection of Residues in the NMDA Receptor NR1 and NR2A Subunits. In the GluR2 X-ray structures, five residues (LB1–5) directly coordinate bound ligands through hydrogen bonds. Amino acids at equivalent positions were targeted by cysteine-substitution mutagenesis in the NMDAR NR1 and NR2A subunits (Fig. 2). The residue at

position LB4 is of special interest. In GluR2, LB4 is Thr655, which forms a hydrogen bond with the γ-carboxylate oxygen of the ligand glutamate. In the glycine-binding site formed by the NMDAR NR1 subunit, Val689 occupies the LB4 position. Its hydrophobic side chain cannot act as a hydrogen donor or acceptor, and it acts to prevent L-glutamate from binding to the glycine binding site and accommodates the much smaller ligand glycine (Furukawa and Gouaux, 2003). Because no X-ray structure is available for the LBD of the NR2A subunit, amino acids corresponding to LB1–5 were identified by amino acid alignment with GluR2 and NR1. Table 1 provides the expression levels for the mutants.

Three additional positions were studied that may play critical roles in ligand binding but whose side chains are not predicted to coordinate bound ligand. A proline that coordinates ligands through its backbone carbonyl is conserved between GluR2 (Pro478) and NR1 (Pro516) but is substituted to Ser511 in NR2A. Ile691 in NR1, positioned at the interlobe interface, was identified as a critical residue in an initial screen. Finally, Tyr450 in GluR2 functions as a "lid" by sterically preventing bound ligand from leaving the closed-cleft conformation. This residue is substituted to Phe484 in NR1 and to His485 in NR2A.

Effect of MTSEA on Wild-Type NMDA Receptors. The NMDAR NR1 and NR2A subunits employed in this study contain many cysteine residues in their extracellular domains, including several in the LBDs. The effect of MTSEA modification on wild-type NMDAR agonist sensitivity was therefore investigated first. MTSEA treatment had no effect on the maximal response of wild-type NMDA receptors to saturating concentrations of the full agonists glycine and L-glutamate (Fig. 3). To determine whether MTSEA treatment altered the affinity or efficacy of the wild-type receptor, modification-induced changes in K_A and E were calculated for partial agonists of the glycine and glutamate binding sites. D-serine evokes a maximum response that is indistinguishable from that of glycine and is therefore a full agonist

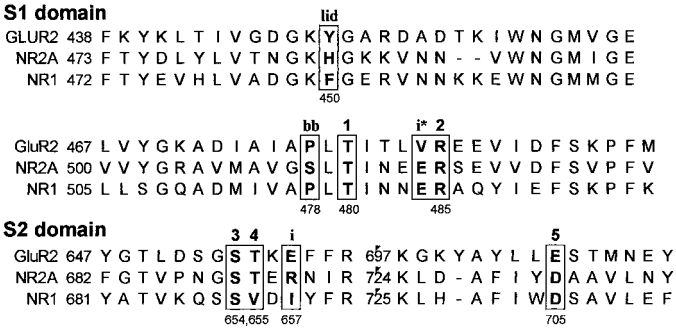

Fig. 2. Sequence alignment of the ligand-binding domains of GluR2, NR1, and NR2A. Shown are regions of the S1 and S2 lobes that contain amino acids critical for ligand binding. Numbers 1 to 5 designate the residues in which side chains form hydrogen bonds with ligands in the NR1 and GluR2 structures, as well as their homologs in NR2A. These positions are referred to as LB1–LB5 in the text. The amino acid at position LB4 in NR1 (Val689) is an exception, because it does not form a hydrogen bond with glycine. The amino acid at the position indicated with the letters bb (Pro499 in GluR2) contributes to ligand binding through its backbone carbonyl, which forms a hydrogen bond with bound ligands (Armstrong et al., 1998). The amino acid at the position indicated with lid forms a lid over ligand bound in the interlobe cleft (Armstrong et al., 1998). The letter i denotes position Ile691 in NR1, which when mutated to cysteine forms an interlobe hydrogen bond with the residue E522 at position i*. The high degree of amino acid conservation allows for a nonambiguous alignment of the NR2A sequence.

at the glycine site in the wild-type NMDAR. This agonist was included because it acted as a partial agonist in some of the cysteine substitution mutants. D-cycloserine, a partial agonist at the glycine site, has an intrinsic activity (α) of 0.81 in the wild-type receptor. The affinity (K_A) and efficacy (E) for D-cycloserine were not altered by MTSEA treatment. The effects of MTSEA modification were also examined for partial agonists at the glutamate site (Fig. 3b). MTSEA treatment resulted in a small but statistically significant reduction of K_A and E for L-aspartate ($\alpha = 0.91$) but did not change K_A or E for NMDA ($\alpha = 0.79$).

Partial Agonists Reveal Efficacy-Induced Changes in EC_{50}. An initial screen for activation phenotypes in the NR1 ligand binding domain identified a cysteine mutant, I691C, in which MTSEA modification dramatically increased the EC_{50} for the full agonist. A glycine concentration-response curve generated for NR1 I691C revealed a left-shifted phenotype relative to the wild-type receptor. After treatment with MTSEA, the EC_{50} increased without a significant effect on the maximal response (Fig. 4a). It was not possible to evaluate, using the full agonist glycine, whether the EC_{50} shift was caused by a change in affinity, a change in efficacy, or both. The effect of MTSEA treatment on the response to the partial agonist D-cycloserine (DCS) was evaluated for receptors containing NR1 I691C. MTSEA modification induced an increase in the EC_{50} and a reduction in maximal response to DCS (Fig. 4, c and d). The EC_{50} shift arose solely from a decrease in efficacy, because there was no significant change in the affinity constant K_A. These results illustrate the fact that a shift in EC_{50} does not necessarily represent a change in affinity. The reduction in maximal response to DCS suggests that modifying the side chain of I691 affects efficacy alone. The lack of reduction in maximal response to glycine is not inconsistent with an efficacy mutation (Colquhoun, 1998), but instead demonstrates the utility of partial agonists as a more sensitive assay for changes in efficacy.

Characterization of Ligand-Binding Residues in the NMDA Receptor. Structures of the GluR2 ligand binding core reveal that all cocrystallized ligands form hydrogen bonds with the sidechains of the same set of five residues (Armstrong and Gouaux, 2000; Mayer et al., 2001; Jin et al., 2002; Jin and Gouaux, 2003). The amino acid ligands and their synthetic derivatives are held in the binding pocket through interactions with their α-carboxyl and α-amino groups. This pattern of coordination suggests that these residues attract ligands to the binding site by a common mechanism. The coordination mechanism observed in GluR2 is conserved among glutamate receptor subunits, as shown by the recent structure for the ligand binding core of the NMDAR NR1 subunit (Furukawa and Gouaux, 2003).

Cysteine residues were introduced at each of the five putative ligand-binding positions in both NR1 and NR2A. For ease of identification and comparison, these positions are designated LB1–5 (see Fig. 2 for residue names). Positions 1 and 2 are located on the S1 lobe of the LBD, whereas positions 3 to 5 are located on the S2 lobe. Because functional NMDA receptors are heteromeric assemblies of NR1 and NR2A subunits, mutations were introduced into each subunit separately and coexpressed in *X. laevis* oocytes with the complementary wild-type subunit. Seven of the 10 mutants supported NMDA currents. However, cysteine substitution

at position LB3 in either NR1 (S688C) or NR2A (S689C) resulted in a nonfunctional receptor, as did the mutation at position LB5 in NR2A (D731C).

Concurrent Affinity and Efficacy Phenotypes in NR2A. Selected residues in the L-glutamate binding site in the NMDAR NR2A subunit were individually mutated to cysteine (Fig. 2). Functional NR2A subunits containing these cysteine substitutions were characterized by concentration-response analysis. To determine the identity of the full agonist for the glutamate site of each mutant, complete concen-

TABLE 1
Expression levels of NMDA receptor mutants
Average NMDA currents before and after MTSEA modification are provided. The number of oocytes (*N*) is provided in Table 2.

	Mutant	Agonists		Average Current Size	
		Full	Partial	Before	After
				nA	
NR1	T518C	Gly	D-Ser	13,200	13,800
NR2	T518C	Gly	DCS	540	101
NR1	R523C	D-Ser	DCS	7800	2400
NR2	R523C	D-Ser	Gly	1312	240
NR1	V689C	Gly	D-Ser	7080	180
NR2	V689C	Gly	DCS	16,800	738
NR1	D732C	Gly	D-Ser	6600	6600
NR2	D732C	Gly	DCS	10,800	6000
NR2A	T513C	L-Glu	NMDA	13,800	9600
NR2A	R518C	L-Glu	D-Glu	1188	2020
NR2A	T690C	L-Asp	L-Glu	4800	203
NR1	I691C	Gly	DCS	1079	603
NR2A	H485C	L-Glu	NMDA	1800	209
NR2A	S511C	L-Glu	L-Asp	6000	540

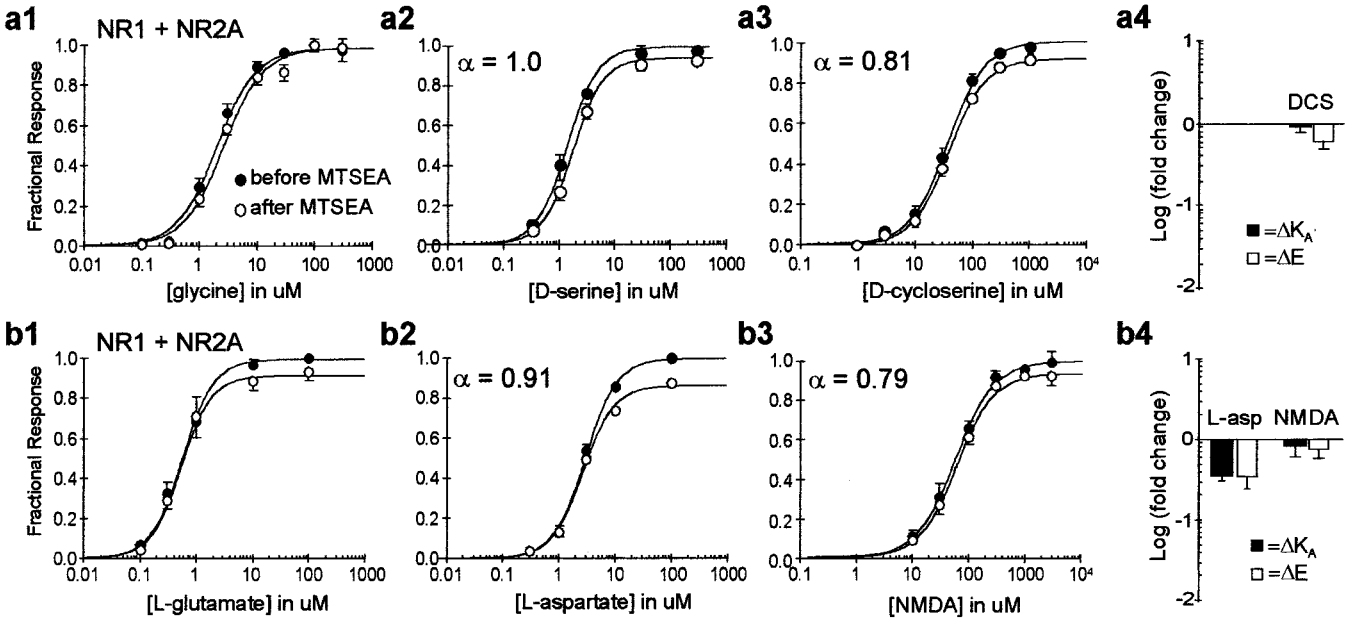

Fig. 3. Effect of MTSEA treatment on NMDA receptor concentration-response curves. a, effect of MTSEA treatment on the concentration-response relationships in wild-type NMDA receptors, for glycine site agonists. Data are shown for two full agonists, glycine (a1) and D-serine (a2), as well as a partial agonist, DCS, which has an intrinsic activity (α) of 0.81 (a3). MTSEA treatment has no significant effect on the affinity or efficacy constants for the glycine binding site in the wild-type receptor (a4). b, effect of MTSEA treatment on concentration-response relationships in wild-type NMDA receptors, for glutamate site agonists. Data are shown for the full agonist L-glutamate (b1) and two partial agonists, L-aspartate (b2) and NMDA (b3). Intrinsic activities (α-values) are indicated for partial agonists. MTSEA treatment has no significant effect on the affinity or efficacy constants for glutamate binding site of the wild-type receptor (b4). Concentration-response relationships were generated for wild-type NR1+NR2A NMDA receptors, before and after a 1-min treatment with 0.5 mM MTSEA. ●, responses in untreated oocytes; ○, responses recorded after MTSEA treatment. All responses are normalized using the response to a saturating concentration of agonist determined before MTSEA treatment. Concentrations of full or partial agonist were coapplied with a saturating concentration of the full agonist at the complimentary subunit of the receptor.

tration-response curves were obtained for various glutamate site agonists (Fig. 5). Glutamate elicited the largest response in T513C (LB1) and R518C (LB2), but L-aspartate was the most efficacious agonist in T690C (LB4). Introduction of a cysteine at position LB2 (R518C) produced an extremely right-shifted phenotype, consistent with results published previously (Uchino et al., 1992; Wafford et al., 1995; Kawamoto et al., 1997). Because the efficacy (E-value) of L-glutamate is not known, it is not possible to evaluate whether this shift is caused by a change in affinity or efficacy. To determine whether the mutated positions displayed an efficacy phenotype, the effect of MTSEA modification on the maximum response was examined. Modification decreased the maximal response for two mutants, consistent with a decrease in efficacy, but increased the maximal response for R518C. It is tempting to speculate that the positive charge of the original arginine residue is important for efficacy, in that modification of the substituted cysteine by MTSEA, which is positively charged, increased current amplitude.

The full agonist data allowed us to qualitatively assign efficacy phenotypes to the three mutated positions, but partial agonist concentration-response data are necessary to obtain more quantitative information about the roles of these residues. The effects of MTSEA on partial agonist EC_{50} values and maximal responses were measured to calculate the fold change in E and K_A. Figure 5 shows that LB1 (T513C), LB2 (R518C), and LB4 (T690C) displayed efficacy phenotypes consistent with the full agonist results. However, all three positions also exhibit affinity phenotypes, indicated by significant changes in the affinity constant K_A (Fig. 5; Table 2). These results suggest that ligand-binding residues may exercise concurrent roles in affinity and efficacy.

Dual-Role Phenotypes Are Conserved in NR1. To determine whether the concurrence of affinity and efficacy phenotypes is conserved between the NMDA subunits, the cysteine modification approach was applied to NR1. As in NR2, MTSEA modification altered the maximal response to the full agonist in all four functional NR1 mutants (Fig. 6). Modification did not significantly alter the EC_{50} in any of the four mutants. If modification altered only agonist efficacy, a change in the EC_{50} would be expected as well. However, the lack of change in the EC_{50} might arise from a concurrent increase in affinity, which would decrease the EC_{50}. To evaluate the possibility that the mutated positions had roles in affinity, the concentration-response series were repeated using partial agonists. In this group of mutants, we elected to compare the results of two distinct partial agonists at each mutant. This was done to determine how the observed phenotypes depended on the intrinsic activity of the agonist and their chemical structure. As in NR2, all positions tested displayed both affinity and efficacy phenotypes. In receptors containing R523C, V689C, or D732C, concurrent affinity and

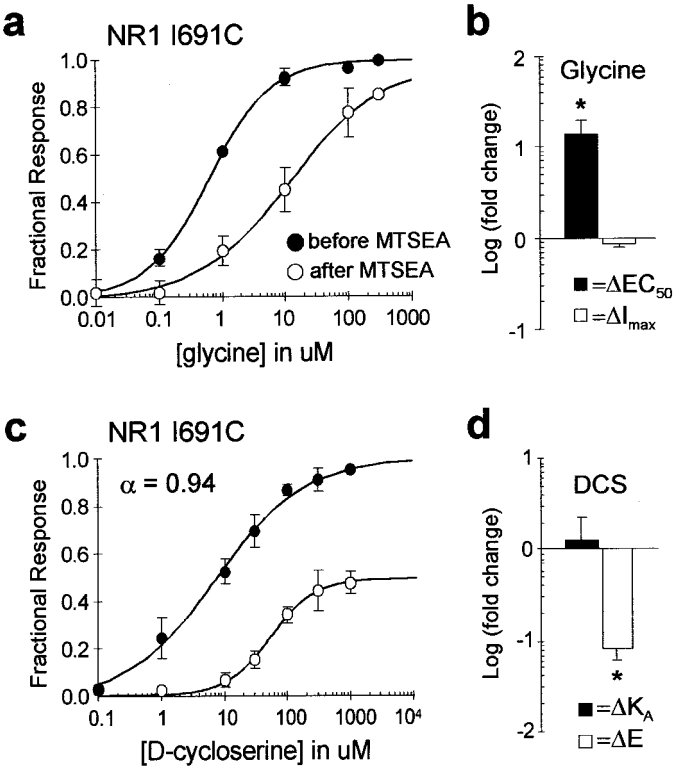

Fig. 4. Partial agonist reveals efficacy phenotype underlying EC_{50} shift. a and b, MTSEA treatment of receptors composed of NR1-I691C + wild-type NR2A induced an increase in the EC_{50} for the full agonist glycine. There was no effect on the maximum response. c and d, the EC_{50} shift induced by modification of I691C is caused by a reduction of efficacy. MTSEA modification of NR1 I691C increased the EC_{50} and reduced the maximal response to the partial agonist DCS. The intrinsic activity of DCS and modification-induced changes in EC_{50} and maximal response were used to calculate changes in E and K_A. Although E was significantly reduced, there was no effect on K_A.

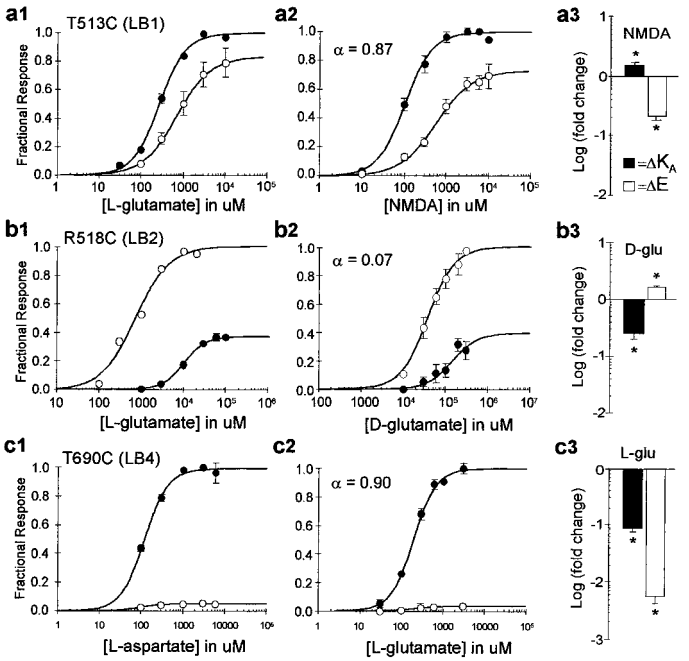

Fig. 5. Affinity and efficacy contributions of ligand-binding residues in NR2A. Concentration-response relationships were determined, before and after MTSEA treatment, for the three functional ligand binding site mutants LB1 (T513C), LB2 (R518C), and LB4 (T690C) in NR2A. The analysis was performed for a full agonist (column 1) and a partial agonist (column 2). a, MTSEA modification reduced the modification of NR2; T513C decreased E and increased K_A for the partial agonist NMDA. b, modification increased the maximal response of NR2-R518C to the full agonist L-glutamate. It also decreased the L-glutamate EC_{50}. Modification of NR2-R518C decreased K_A and increased E for the partial agonist D-glutamate. c, modification severely reduced the maximal response of NR2-T690C to L-aspartate, which generated the largest response and is therefore designated the full agonist in this mutant. Modification of NR2 T690C decreases both K_A and E of the partial agonist L-glutamate.

efficacy phenotypes were observed for both partial agonists tested (Table 2). However, T518C demonstrated both affinity and efficacy phenotypes when tested with D-serine, but an affinity-only phenotype when tested with D-serine. Taken collectively, the results in NR1 suggest that the majority of coordinating positions have little agonist specificity in their roles, whereas position LB1 (T518C) may differentiate between agonists by interacting with nonconserved moieties of glycine site agonists.

Unlike its counterpart in GluR2, residue Val689 at the LB4 position in NR1 does not form a hydrogen bond with bound glycine (Furukawa and Gouaux, 2003). Nonetheless, a combined affinity-efficacy phenotype was found for the V689C mutation, for both partial agonists, DCS and D-serine. The side chain of the wild-type valine residue cannot act as a hydrogen donor, and the full agonist glycine is missing the γ-carboxylate oxygen of L-glutamate. However, the thiol group of the substituted cysteine in V689C may be able to form a hydrogen bond with the hydroxyls of the two partial agonists DCS and D-serine. The phenotype of this mutation suggests that this in fact occurs.

Noncoordinating Residues Do Not Contribute to Affinity. A number of amino acid positions were identified that may play a critical role in ligand binding but in which sidechains do not directly coordinate any of the ligands cocrystallized with the NR1 or GluR2 ligand binding domain (Armstrong and Gouaux, 2000; Furukawa and Gouaux, 2003). One of these, NR1-Ile691, resides at the interlobe interface and has been described above (Fig. 4). Two additional noncoordinating residues were characterized by the covalent modification approach. NR2A residue Ser511 corresponds to Pro499 in GluR2 and Pro516 in NR1, which contribute to ligand binding by forming a hydrogen bond to the bound agonists with their backbone carbonyl oxygen. MTSEA modification of S511C decreased the efficacy constant E for L-aspartate but had no significant effect on affinity (Fig. 7). This phenotype was also observed for H485C. His485 is located in the S1 lobe of NR2A and forms a hydrogen bond with Pro686 of the S2 lobe. This interlobe hydrogen bond is associated with the closed forms of the LBD that are induced by high-efficacy agonists. Therefore, modification of H485C decreases the efficacy constant E for L-aspartate but does not affect affinity (Fig. 7). From these results, it seems that noncoordinating residues have roles in efficacy alone.

Model Dependence of Affinity Estimates. The approach described here uses experimentally determined values (intrinsic activity, maximum response, EC_{50}) to estimate affinity and efficacy constants K_A and E. The relationship between these experimental parameters and the desired constants depends on the underlying model. We therefore investigated the sensitivity of the approach to changes in the underlying kinetic model. As an alternative to the linear three-state del Castillo-Katz model, a model was chosen that uses two identical and independent binding sites (Fig. 1b). Because the NMDAR contains two glycine and two L-glutamate binding sites, this model is more realistic than the one-site model. Because two of the four binding sites are always saturated in the experiments described here, a two-side model seems appropriate. The efficacy constant E is not altered in the two-site model, but the affinity-dependent equilibrium dissociation constant K_A is quite different (Fig. 1b). In fact, the K_A values for the 2-site model were between 3- and 5 times smaller than the corresponding values for the 1-site model. However, the relevant parameter here is not the absolute value of K_A but the *change* in the K_A value resulting from MTSEA treatment. Figure 8 illustrates the effect of altering the underlying model on the fold-change in K_A for the mutations tested. Despite the significant effect on the absolute value of K_A, the ratios of K_A values before and after MTSEA treatment were remarkably insensitive to the details of the underlying model. In fact, the assignment of affinity-efficacy roles to individual positions was identical for the 1- and 2-site models.

TABLE 2

Summary of phenotypes at ligand-binding positions in NR1 and NR2.

Affinity and efficacy phenotypes for the 10 cysteine substitutions described in this article. The ID column tabulates the structural role of the mutated amino acids: LB1–LB5 are residues in which sidechains form hydrogen bonds with the bound ligand in the GluR2 crystal structure. The position labeled 'lid' sterically prevents the bound ligand from leaving the closed cleft conformation. The amino acid labeled 'bb' forms an H-bond between its backbone carbonyl oxygen and the bound ligand. The position labeled 'i' refers to a residue at the interlobe interface. For each position, the following information is tabulated: which compound was a full agonist at the Gly site (in NR1) or glutamate site (in NR2A); which partial agonists were used; the fold-change in affinity constant KA and efficacy constant E (mean ± S.E.M., *P*-value). Significant *P*-values ($P < 0.05$) are shown in bold. The rightmost column lists which phenotype was found.

			Agonist				Fold Change K_A		Fold Change E		
	Mutant	ID	Full	Partial	α	*N*	Mean ± S.E.M.	*P*	Mean ± S.E.M.	*P*	Role
	Wild-type		Gly	DCS	0.81	9	−1.2 ± 0.6	0.23	−1.6 ± 0.7	0.061	N.A.
			Gly	D-Ser		4	1.2 ± 0.07	0.035	0.6 ± −1.6	0.039	
			L-Glu	L-Asp	0.91	6	−2.9 ± 0.7	**0.03**	−3.6 ± 1.2	**0.04**	N.A.
			L-Glu	NMDA	0.79	5	−1.3 ± 0.9	0.21	−1.8 ± 0.5	0.155	N.A.
NR1	T518C	LB1	Gly	DCS	0.44	9	−3.0 ± 0.6	**0.002**	−17.2 ± 5.2	**0.000**	A,E
				D-Ser	0.81	12	22.8 ± 6.2	**0.008**	1.0 ± 0.7	0.770	A
NR1	R523C	LB2	D-Ser	DCS	0.88	7	−2.1 ± 0.2	**0.008**	−17.0 ± 4.3	**0.0004**	A,E
				Gly	0.76	4	−17.1 ± 5.6	**0.04**	−29.7 ± 13.1	**0.04**	A,E
NR1	V689C	LB4	Gly	DCS	0.75	5	−4.3 ± 0.4	**0.0003**	−51.5 ± 7.2	**0.0004**	A,E
				D-Ser	0.88	3	−7.6 ± 0.6	**0.002**	−273 ± 67	**0.002**	A,E
NR1	D732C	LB5	Gly	DCS	0.88	3	−87.3 ± 57.5	**0.0001**	−9.9 ± 4.0	**0.001**	A,E
				D-Ser	0.81	8	−10.0 ± 5.1	**0.002**	−3.3 ± 0.5	**0.010**	A,E
NR2A	T513C	LB1	L-Glu	NMDA	0.91	5	1.5 ± 0.6	**0.03**	−5.1 ± 0.7	**0.022**	A,E
NR2A	R518C	LB2	L-Glu	D-Glu	0.01	4	−5.3 ± 2.4	**0.04**	1.7 ± 0.1	**0.004**	A,E
NR2A	T690C	LB4*	L-Asp	L-Glu	0.90	6	−11.8 ± 2.0	**0.003**	−213 ± 54	**0.001**	A,E
NR1	I691C	i	Gly	DCS	0.94	4	1.2 ± 1.2	0.55	−23.4 ± 0.0	**0.001**	E
NR2A	H485C	lid	L-Glu	NMDA	0.46	3	−2.0 ± 0.7	0.35	−11.3 ± 3.0	**0.010**	E
NR2A	S511C	bb	L-Glu	L-Asp	0.47	7	−2.1 ± 0.2	0.52	−20.6 ± 3.6	**0.023**	E

A, affinity, E, efficacy, N.A., not applicable.

Discussion

Receptors recognize ligands with a high degree of specificity by employing a binding site whose three-dimensional structure and physicochemical properties exactly complement those of the appropriate agonist. The accuracy of the structural fit determines the number of favorable interactions allowed to form between the ligand and its binding site. This structural complementarity is an important determinant of a ligand's affinity for its receptor. A second fundamental property, efficacy, is required to account for the existence of partial agonists and competitive antagonists. Efficacy measures the degree to which a ligand is able to activate the receptor. Both affinity and efficacy are required to fully characterize the ligand-receptor interaction. The exact molecular determinants of agonist affinity and efficacy have remained poorly understood, in large part because of the absence of methods to empirically quantify these properties. We have attempted to address this problem by measuring changes in concentration-response curves of full and partial agonists induced by covalent modification of introduced cysteines. The approach was applied to define the molecular attributes that control affinity and efficacy in both NR1 and NR2A subunits of the NMDA receptor.

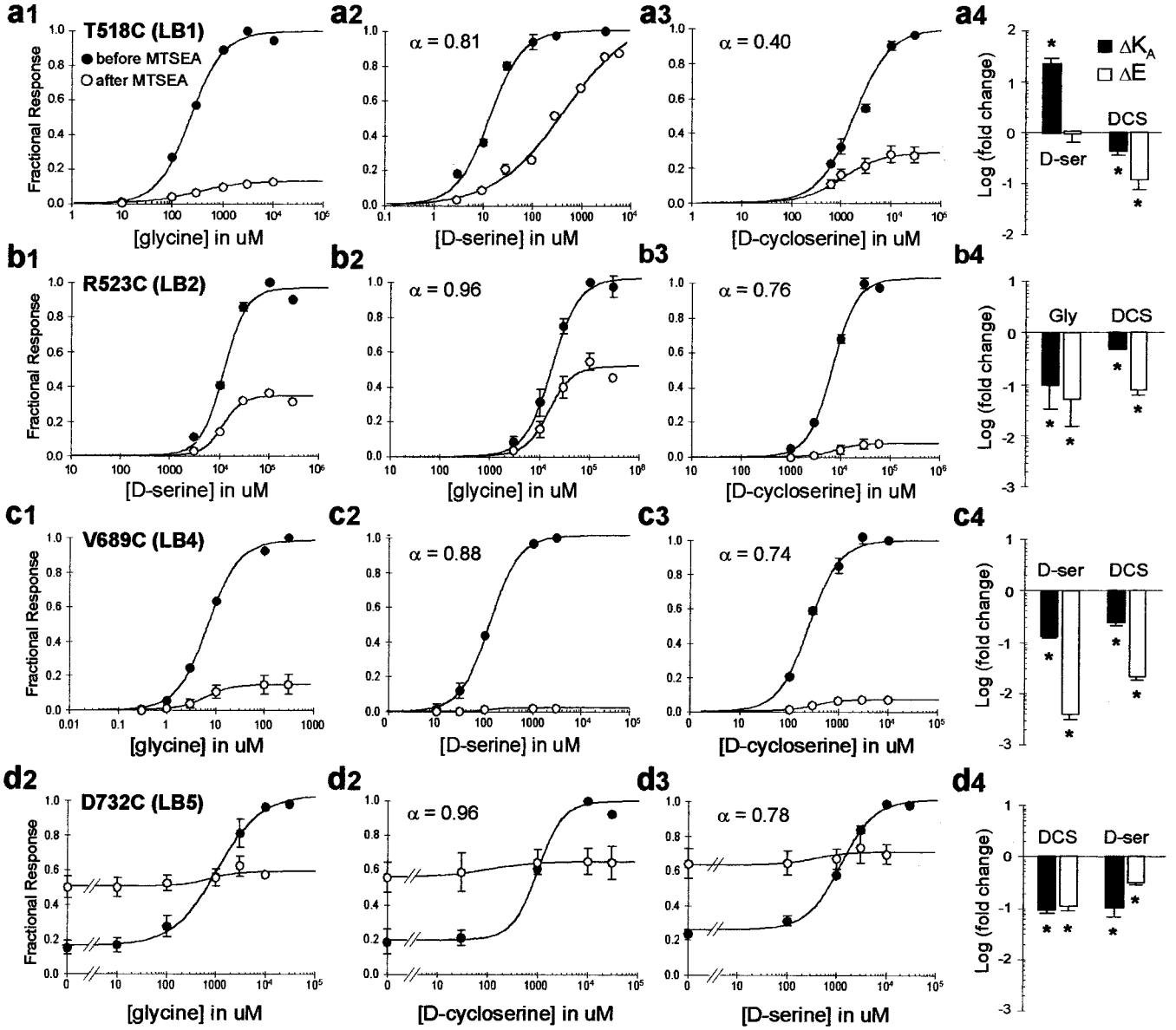

Fig. 6. Affinity and efficacy contributions of ligand binding residues in NR1. a, MTSEA modification reduced the maximal response of NR1-T518C to glycine. Modification increased K_A but not E for partial agonist D-serine. For the partial agonist DCS, modification significantly decreased both K_A and E. b, MTSEA modification reduced the maximal response of NR1-R523C to D-serine, which generated the largest response in this mutant and is therefore designated the full agonist. Modification decreased both K_A and E for glycine, a partial agonist in this mutant. Modification also decreased both K_A and E for DCS. c, MTSEA modification reduced the maximal response of NR1-V689C to the full agonist glycine. Modification decreases both K_A and E for the two partial agonists D-serine and DCS. d, MTSEA modification reduced the maximal response of NR1-D732C to the full agonist glycine. For the partial agonists D-serine and DCS, modification decreases both K_A and E. The pronounced ability of glutamate alone to activate the receptor after MTSEA modification is attributed to the partial positive charge of the conjugated MTSEA moiety. This charge may substitute for the α-amino group of glycine, which is predicted to interact with the native D732 residue.

Limitations of the Approach. The method used in this study requires that a cysteine be introduced at the position that is investigated. The position is further altered by thiol modification of the cysteine side-chain, and the effect of this modification on receptor function is evaluated. Therefore, the same position is mutated twice, first to cysteine and then by thiol modification. Only the second phase provides data on the role of the mutated position in affinity and efficacy. Herein lies the major limitation of the approach: the affinity and efficacy changes are measured by effects of MTSEA modifications performed in a mutant background. As long as the cysteine substitution produces only a relatively small effect on ligand-receptor interaction, this may be an acceptable problem. In several instances, the cysteine substitution proved to be incompatible with NMDAR function: of the 10 cysteine substitutions targeting the LB1-LB5 positions, three resulted in loss of function. No NMDA currents could be detected when cysteines were introduced at LB3 in either NR1 (Ser688) or NR2A (Ser689), or at LB5 in NR2A (Asp732), eliminating these positions from the analysis. Even when a cysteine substitution is functional, it could produce a major change in agonist potency and a maximal change in affinity and/or efficacy. Such a mutant may not demonstrate further alteration of function upon MTSEA treatment, limiting the ability to evaluate the effects of modification. Because MTSEA treatment of all functional mutants at ligand-coordinating residues produced significant alterations in both affinity and efficacy, the introduction of a cysteine did not completely eclipse the ability of thiol modification to reveal phenotypes. However, there could be more subtle complications: the effect of a cysteine substitution on agonist affinity or efficacy could alter the subsequent effect of MTSEA on these parameters.

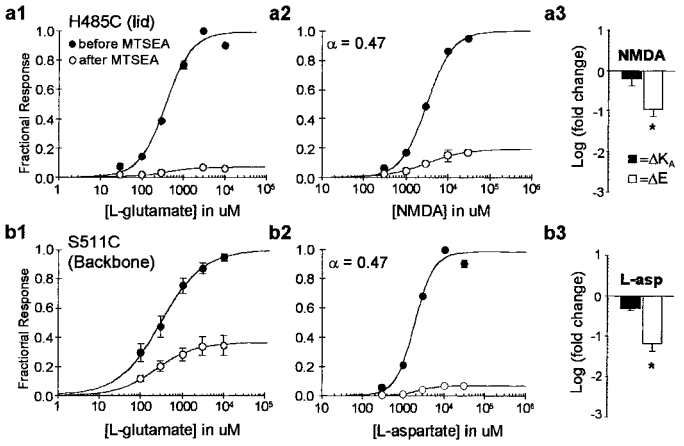

Fig. 7. Pure efficacy phenotypes in noncoordinating residues in NR2A. a, modification of NR2-H485C decreased maximum response but not EC_{50} for the full agonist L-glutamate. Modification decreased E, but has no effect on K_A for NMDA. b, MTSEA modification of NR2-S511C did not change EC_{50} but reduced maximum response to the full agonist L-glutamate. Modification decreased E but not K_A for L-aspartate.

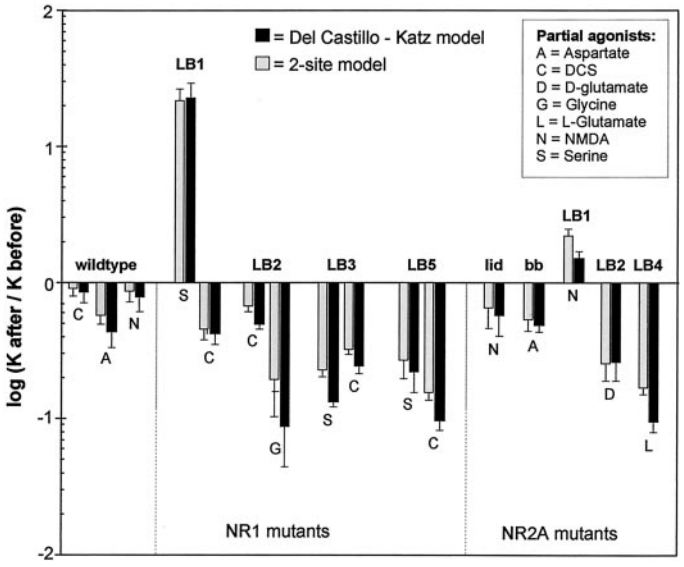

Fig. 8. Effect of underlying model on estimated change in affinity constant. The calculation of K_A requires that a specific kinetic model is assumed to underlie the data. One clear limitation of the del Castillo-Katz model is the assumption of a single binding site. Because NMDA receptors contain two binding sites for each of the two coagonists L-glutamate and glycine, an alternative model employing two equivalent binding sites (Fig. 1b) was evaluated as well. Estimates for K_A are substantially different between the 1- and 2-site models (Fig. 1b). However, as the figure illustrates, the ratio of the K_A before and after MTSEA modification is virtually the same for most mutants.

Selection of Residues in the Ligand Binding Domain. Using the crystallized ligand binding core of GluR2 as a structural model, eight positions were selected for mutation in the NMDAR NR1 and NR2A subunits, based on their potential roles in agonist binding and transduction (Fig. 2). The sidechains of five of these positions (LB1–5; Fig. 2) form a coordinating hydrogen bond network with bound ligand. Three positions were targeted in which amino acids were predicted to play critical roles in affinity or efficacy but side chains do not directly coordinate agonists. The noncoordinating amino acids studied include NR1-Ile691, which is located at the S1-S2 interface; NR2A-His485, which is predicted to interact with ligand through its backbone carbonyl; and NR2A-Ser511, which is predicted to form a "lid" on the binding cleft. Cysteine substitution of the backbone position in NR1 (P516C) was lethal, whereas mutation of the "lid" position in NR1 (F484C) resulted in an NMDAR that was nearly fully activated by L-glutamate alone, which prevented characterization of the glycine binding properties. The remaining 10 functional cysteine substitutions were characterized by the thiol-modification approach, using both full and partial agonists at the glycine and glutamate sites.

Partial Agonists Reveal Affinity-Efficacy Contributions to Mutant Phenotypes. The importance of using partial agonists was illustrated by the NR1 mutant I691C, for which MTSEA modification shifted the dose-response curve for the full agonist glycine without affecting maximum response (Fig. 4ab). Because the glycine EC_{50} depends on both K_A and E (Fig. 1 and *Materials and Methods*), MTSEA modification could have affected affinity, efficacy or both. It is therefore impossible to unambiguously interpret this result. Repeating the experiment using the partial glycine site agonist DCS resolves this issue: MTSEA modification clearly affects the maximum response for DCS, reducing the intrinsic activity from 94% to 45%. The observed right-shift in the EC_{50} is entirely attributed to a reduction of efficacy, with no statistically significant effect on affinity (Fig. 4, c and d). Analysis of the NR1 crystal structures (Furukawa and Gouaux, 2003) revealed that residue Ile691 is located in the S2 lobe at the S1-S2 interface. Mutating the isoleucine at position 691 to cysteine introduces a novel interlobe hydro-

gen bond with residue Glu522 in S1 (Fig. 9). The Cys691-Glu522 H-bond is present only in the structure containing the full agonist glycine: the distance between the atoms forming the H-bond increases to 10.7 Å in the structure containing the antagonist 5,7-dichlorokynurenic acid. The structural analysis explains the leftward shift of the glycine concentration-response curve: the I691C mutation increases the glycine efficacy by allowing one additional interlobe H-bond to form when the LBD closes after glycine binding. It also helps explain the pure efficacy phenotype caused by subsequent modification of the thiol at position 691 by MTSEA: the bulky moiety introduced here would interfere sterically with complete domain closure and thereby reduce the stability of the closed-cleft conformation.

Coordinating Residues Control Both Affinity and Efficacy. All 10 functional cysteine substitutions studied were found to make significant contributions to efficacy. However, affinity phenotypes were limited to positions in which side chains formed hydrogen bonds with bound ligands. Although all of the functional coordinating residues contributed to both affinity and efficacy, phenotypes of the backbone (bb), interface (i), and lid residues were limited to efficacy alone. Together, our results show that affinity and efficacy are distinct, quantifiable measures of the physical processes of binding and transduction. The absolute concurrence of affinity and efficacy phenotypes in the coordinating residues indicates that they play a dual role: 1) recruitment of ligands to the open binding cleft and 2) initiation of a conformational change of the LBD, cleft closure, that culminates in receptor activation.

Efficacy, Gating, and Open Probability. In the 1957 del Castillo-Katz model (Fig. 1a), there are only two coupled equilibria, describing ligand binding and channel opening (gating). In this simplistic model, agonist efficacy results from channel opening; consequently, a channel's maximum open probability (P_o) can be employed to calculate the efficacy constant E (Fig. 1a and *Materials and Methods*). However, a single conformational change is not sufficient to describe receptor activation in ligand gated ion channels. The binding cleft closure induced by agonist binding is the first step in a cascade of events that culminates in channel opening. In models with more than one gating step, the maximal open probability depends on all the individual steps in the transduction pathway (Fig. 1e). The gating machinery described by the final step in the cascade maps the open-cleft/closed-cleft behavior of the binding site to a possible range of open probabilities. Even when the binding site is completely and stably closed, because it is occupied by a full agonist, the associated channel will continue to gate with an open probability (P_o) that is determined by intrinsic properties of the pore-forming domain. The actual value of P_o is set by the gating machinery; therefore, it can be altered by mutations in the gate (Akabas et al., 1994). As a result, even full agonists with very high E-values can produce low open probabilities. The maximum open probability for the NMDA receptor is relatively low, but this does not imply that the efficacy of glycine and L-glutamate is small. In fact, glycine efficacy must be quite large, because glycine completely protects the NR1-A714C mutant from being modified by the thiol-modifying reagent dithionitrobenzoate by efficiently stabilizing the closed cleft conformation (Wood et al., 1997). The efficacy of L-glutamate is likely to be even higher then that of glycine because its side chain atoms can form addition stabilizing interactions with the closed form of the LBD.

A reasonable estimate for the efficacy constant E can only be made for partial agonists. The estimate relies on measuring the intrinsic activity of the agonist, which is equivalent to

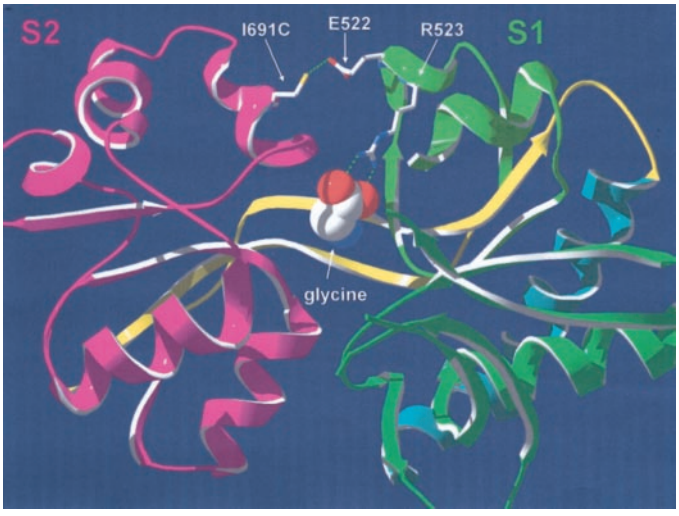

Fig. 9. Mutation NR1 I691C introduces a novel interlobe hydrogen bond. The structures of the ligand-binding domain of NR1 with various ligands (accession numbers 1bp7, 1bp8, 1bp9, and 1bpQ in the Brookhaven database) were analyzed using SwissPDBViewer (Guex and Peitsch, 1997). Coloring is as follows: S1 is green, most of S2 is pink, the hinge region is yellow, and helix J (a part of S2 below S1) is cyan. Ile691 in NR1 is located in the S2 lobe at the S1-S2 interface, near Glu522, is S1. Introducing Cys691 in the structure containing glycine (1pb7.pdb) predicts the formation of a putative novel interlobe hydrogen bond between Cys691 and Glu522, as illustrated in the image. The length of the hydrogen bond is 3.21 Å. This distance increases to 10.7 Å in the structure containing the antagonist 5,7-dichlorokynurenic acid (1pbq.pdb).

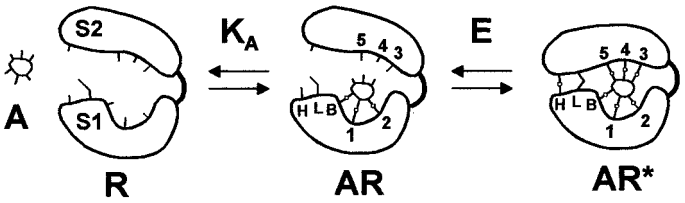

Fig. 10. Molecular determinants of affinity and efficacy in the NMDA receptor. Amino acids in the ligand-binding domains of NR1 and NR2A that are predicted to coordinate bound ligands were targeted by a mutagenesis approach that allows assignment of affinity and efficacy phenotypes. All functional mutants in which side chains are predicted to form H-bonds with bound ligands seem to have both affinity and efficacy roles. To understand the molecular implications of these findings, a microscopic version of the del Castillo-Katz model for activation of ligand-gated ion channels (Fig. 1a) was applied to a structural model of a ligand-binding domain of the NMDA receptor. The cartoons show a schematic representation of the agonist (A), as well as the receptor (R), in three different conformations. The two globular lobes, S1 and S2, are shown connected by a hinge. The diagram on the left shows the unoccupied receptor (R) in an open-cleft conformation, whereas the diagram on the right shows the ligand-bound closed-cleft conformation (AR*). No crystal structure exists for the middle cartoon (AR), which represents a transition state in which ligand has bound to the open-cleft conformation, but no conformational change of the receptor has yet occurred. Although ligand is depicted as bound to three residues in S1, our data indicate that ligand may be able to initially interact with residues on either or both lobe(s). Side chains critical for ligand binding are indicated as follows: numerals 1 to 5, residues predicted to directly coordinate ligand through their sidechains; L, lid-forming residue (see Fig. 2); B, residue that coordinates ligand through its backbone carbonyl; and H, representing a class of residues that form interlobe hydrogen bonds unique to the closed-cleft conformation (Armstrong and Gouaux, 2000).

the normalized open probability. If the activation cascade can be properly described by a linear sequential scheme (Fig. 1e), then the method described here will correctly estimate the value of E (Fig. 1, f and g). However, these linear schemes do not take into account the multisubunit organization of the NMDA receptor, potential interactions between ligand binding cores, or the possibility of receptor activations resulting from occupancy of less then four binding sites. It is conceivable that the estimation of the E-value used here will prove incorrect for more realistic and therefore complex kinetic models. However, it is possible that the *ratio* of E-values before and after MTSEA modification (Fig. 1h) is still a reliable measure for changes in efficacy, just as the K_A ratio is a robust measure for changes in affinity (Fig. 9).

Affinity, Efficacy, Binding, and Conformational Change. Ligand binding to the bilobate GluR2 and NR1 ligand binding domains results in their conversion from an open- to a closed-cleft conformation (Armstrong and Gouaux, 2000; Furukawa and Gouaux, 2003). This process has been proposed to occur in two stages: an initial, rapid association of ligand with the unoccupied binding site, followed by a slower conformational change that stabilizes the ligand-bound structure (Abele et al., 2000). This suggests the existence of an intermediate transition state, in which ligand is bound to the open-cleft conformation. Integrating this idea with the data presented here has prompted us to propose the model shown in Fig. 10. The reversible binding of ligand to the open-cleft conformation (R) is described by the affinity constant, K_A. Our data indicate that both S1 and S2 participate in this initial binding reaction, because residues in both lobes are critical determinants of affinity. The conversion of the agonist-bound open-cleft conformation (AR) to the closed-cleft conformation (AR*) determines agonist efficacy (Fig. 1, e–h). Because all coordinating residues display efficacy phenotypes, each makes a significant contribution to stabilizing the closed-cleft conformation. Additional contributions to efficacy are made by the residues that form interlobe hydrogen bonds (Armstrong and Gouaux, 2000), as well as residues that sterically prevent bound ligand from dissociating, all of which would be expected to shift the $AR \leftrightarrow AR^*$ equilibrium to the right. Our model provides a molecular basis for the strong coupling between binding (affinity) and activation (efficacy) that was initially proposed (del Castillo and Katz, 1957). This model urges a change in how ligand-binding sites are perceived. Rather than forming a static coordinating network, the ligand-binding domain is a dynamic sensor that allows the same five residues to bind ligand and to stabilize the closed-cleft conformation. Efficacy in the NMDA receptor, then, encompasses a series of steps that begins in the ligand-binding domains, continues with movement of the M3 transduction element (Jones et al., 2002), and culminates in channel opening.

References

Abele R, Keinanen K, and Madden DR (2000) Agonist-induced isomerization in a glutamate receptor ligand-binding domain. A kinetic and mutagenetic analysis. *J Biol Chem* **275:**21355–21363.

Akabas MH, Kaufmann C, Archdeacon P, and Karlin A (1994) Identification of acetylcholine receptor channel-lining residues in the entire M2 segment of the alpha subunit. *Neuron* **13:**919–927.

Akabas MH, Stauffer DA, Xu M, and Karlin A (1992) Acetylcholine receptor channel structure probed in cysteine-substitution mutants. *Science (Wash DC)* **258:**307–310.

Ariens EJ (1954) Affinity and intrinsic activity in the theory of competitive inhibition. *Arch Int Pharmacodyn Ther* **99:**32–49.

Arinaminpathy Y, Sansom MS, and Biggin PC (2002) Molecular dynamics simulations of the ligand-binding domain of the ionotropic glutamate receptor GluR2. *Biophys J* **82:**676–683.

Armstrong N and Gouaux E (2000) Mechanisms for activation and antagonism of an AMPA-sensitive glutamate receptor: crystal structures of the GluR2 ligand binding core. *Neuron* **26:**165–181.

Armstrong N, Sun Y, Chen GQ, and Gouaux E (1998) Structure of a glutamate-receptor ligand-binding core in complex with kainate. *Nature (Lond)* **395:**913–917.

Colquhoun D (1998) Binding, gating, affinity and efficacy: the interpretation of structure-activity relationships for agonists and of the effects of mutating receptors. *Br J Pharmacol* **125:**924–947.

del Castillo J and Katz B (1957) Interaction at end-plate receptors between different choline derivatives. *Proc R Soc Lond B Biol Sci* **146:**369–381.

Dingledine R, Borges K, Bowie D, and Traynelis SF (1999) The glutamate receptor ion channels. *Pharmacol Rev* **51:**7–61.

Furukawa H and Gouaux E (2003) Mechanisms of activation, inhibition and specificity: crystal structures of the NMDA receptor NR1 ligand-binding core. *EMBO (Eur Mol Biol Organ) J* **22:**2873–2885.

Guex N and Peitsch MC (1997) SWISS-MODEL and the Swiss-PdbViewer: an environment for comparative protein modeling. *Electrophoresis* **18:**2714–2723.

Jin R and Gouaux E (2003) Probing the function, conformational plasticity and dimer-dimer contacts of the GluR2 ligand-binding core: studies of 5-substituted willardiines and GluR2 S1S2 in the crystal. *Biochem* **42:**5201–5213.

Jin R, Horning M, Mayer ML, and Gouaux E (2002) Mechanism of activation and selectivity in a ligand-gated ion channel: structural and functional studies of GluR2 and quisqualate. *Biochem* **41:**15635–15643.

Jones KS, VanDongen HMA, and VanDongen AMJ (2002) The NMDA receptor M3 segment is a conserved transduction element coupling ligand binding to channel opening. *J Neurosci* **22:**2044–2053.

Kawamoto S, Uchino S, Xin KQ, Hattori S, Hamajima K, Fukushima J, Mishina M, and Okuda K (1997) Arginine-481 mutation abolishes ligand-binding of the AMPA-selective glutamate receptor channel alpha1-subunit. *Mol Brain Res* **47:**339–344.

Leonard JP and Kelso SR (1990) Apparent desensitization of NMDA responses in *Xenopus* oocytes involves calcium-dependent chloride current. *Neuron* **4:**53–60.

Mayer ML, Olson R, and Gouaux E (2001) Mechanisms for ligand binding to GluR0 ion channels: crystal structures of the glutamate and serine complexes and a closed Apo state. *J Mol Biol* **311:**815–836.

Paoletti P, Neyton J, and Ascher P (1995) Glycine-independent and subunit-specific potentiation of NMDA responses by extracellular Mg^{2+}. *Neuron* **15:**1109–1120.

Schorge S and Colquhoun D (2003) Studies of NMDA receptor function and stoichiometry with truncated and tandem subunits. *J Neurosci* **23:**1151–1158.

Stern-Bach Y, Bettler B, Hartley M, Sheppard PO, O'Hara PJ, and Heinemann SF (1994) Agonist selectivity of glutamate receptors is specified by two domains structurally related to bacterial amino acid-binding proteins. *Neuron* **13:**1345–1357.

Sun Y, Olson R, Horning M, Armstrong N, Mayer M, and Gouaux E (2002) Mechanism of glutamate receptor desensitization. *Nature (Lond)* **417:**245–253.

Uchino S, Sakimura K, Nagahari K, and Mishina M (1992) Mutations in a putative agonist binding region of the AMPA-selective glutamate receptor channel. *FEBS Lett* **308:**253–257.

VanDongen AMJ, Frech GC, Drewe JA, Joho RH, and Brown AM (1990) Alteration and restoration of K+ channel function by deletions at the N- and C-termini. *Neuron* **5:**433–443.

Wafford KA, Kathoria M, Bain CJ, Marshall G, Le Bourdelles B, Kemp JA, and Whiting PJ (1995) Identification of amino acids in the *N*-methyl-D-aspartate receptor NR1 subunit that contribute to the glycine binding site. *Mol Pharmacol* **47:**374–380.

Wood MW, VanDongen HMA, and VanDongen AMJ (1995) Structural conservation of ion conduction pathways in K channels and glutamate receptors. *Proc Natl Acad Sci USA* **92:**4882–4886.

Wood MW, VanDongen HMA, and VanDongen AMJ (1997) An alanine residue in the M3–M4 linker lines the glycine binding pocket of the *N*-methyl-D-aspartate receptor. *J Biol Chem* **272:**3532–3537.

Zheng F, Erreger K, Low CM, Banke T, Lee CJ, Conn PJ, and Traynelis SF (2001) Allosteric interaction between the amino terminal domain and the ligand binding domain of NR2A. *Nat Neurosci* **4:**894–901.

Address correspondence to: Antonius M. J. VanDongen, Department of Pharmacology and Cancer Biology, Duke University Medical Center, PO Box 3813, Durham, NC 27710. E-mail: vando005@mc.duke.edu